AIP | Applied Physics Letters

Highly efficient inverted top-emitting green phosphorescent organic light-emitting diodes on glass and flexible substrates

E. Najafabadi, K. A. Knauer, W. Haske, C. Fuentes-Hernandez, and B. Kippelen

Citation: Appl. Phys. Lett. **101**, 023304 (2012); doi: 10.1063/1.4736573
View online: http://dx.doi.org/10.1063/1.4736573
View Table of Contents: http://apl.aip.org/resource/1/APPLAB/v101/i2
Published by the American Institute of Physics.

Highly efficient inverted top-emitting green phosphorescent organic light-emitting diodes on glass and flexible substrates

E. Najafabadi, K. A. Knauer, W. Haske, C. Fuentes-Hernandez, and B. Kippelen
Center for Organic Photonics and Electronics (COPE), School of Electrical and Computer Engineering, Georgia Institute of Technology, Atlanta, Georgia 30332, USA

(Received 5 April 2012; accepted 23 June 2012; published online 11 July 2012)

Green phosphorescent inverted top-emitting organic light-emitting diodes with high current efficacy and luminance are demonstrated on glass and polyethersulfone (PES) substrates coated with polyethylene dioxythiophene-polystyrene sulfonate (PEDOT:PSS). The bottom cathode is an aluminum/lithium fluoride bilayer that injects electrons efficiently into an electron transport layer of 1,3,5-tri(m-pyrid-3-yl-phenyl)benzene (TpPyPB). The cathode is found to be highly sensitive to the exposure of trace amounts of O_2 and H_2O. A high current efficacy of 96.3 cd/A is achieved at a luminance of 1387 cd/m^2 when an optical outcoupling layer of N,N′-Di-[(1-naphthyl)-N,N′-diphenyl]-(1,1′-biphenyl)-4,4′-diamine (α-NPD) is deposited on the anode. © *2012 American Institute of Physics*. [http://dx.doi.org/10.1063/1.4736573]

Organic light-emitting diodes (OLEDs) have attracted significant interest in recent years due to their potential in lighting and display applications. The majority of the research has focused on a device architecture in which the organic layers are sandwiched between a bottom hole-injecting anode and a top electron-injecting cathode.[1,2] These conventional OLEDs are also typically bottom-emitting such that generated light exits the structure through a transparent indium tin oxide (ITO) coated glass anode, leading to undesirable waveguide losses.[3]

In an inverted OLED the injection scheme is reversed so that the cathode is at the bottom of the device and the anode is on top. For an inverted top-emitting OLED the cathode is a highly reflective metallic mirror and the anode consists of either a transparent conductive oxide, such as ITO,[4,5] or a semitransparent thin metal layer.[6,7] For displays, top-emitting OLEDs have the advantage of not requiring a transparent substrate. The device can then be fabricated directly upon its driving circuitry, maximizing the pixel aperture ratio.[8] Moreover, inverted OLEDs are more convenient to integrate with driving electronics based on *n*-type driving transistors.[9] Despite these advantages, reports on inverted top-emitting OLEDs have been rather scarce.[4–7,10–12]

The major challenge of fabricating efficient inverted OLEDs has been finding a highly reflective bottom cathode capable of effectively injecting electrons into the electron transport layer.[9] Most organic semiconductors have a rather low electron affinity making it difficult to inject electrons efficiently from a metal electrode with good environmental stability such as aluminum.[13] Aluminum has a high reflectance and is less reactive than lower work function metals such as calcium and magnesium; however, its work function is too high to be used as an efficient cathode in OLEDs. A strategy that is often employed in conventional top-cathode bottom-emitting OLEDs is to insert a thin layer of lithium fluoride (LiF) between the electron transport layer and the top aluminum cathode.[14] While this approach has been implemented in top-cathode OLEDs, attempts to fabricate bottom cathodes by depositing LiF on top of Al electrodes yielded modest performance with tris-(8-hydroxyquinoline)aluminum (Alq_3)[10,11] electron transport layers.

Reports of inverted top-emitting OLEDs have mostly focused on devices with fluorescent emissive layers.[4–11] The highest current efficacy reported for a fluorescent inverted top-emitting OLED was 33.8 cd/A at 6670 cd/m^2, using an aluminum/lead monoxide cathode.[12] Few attempts have been made to study inverted top-emitting OLEDs with emissive layers containing phosphorescent dopants that allow for both singlet and triplet excited states to contribute to light emission.[7,12] The highest current efficacy reported for a phosphorescent inverted top-emitting OLED was 55.4 cd/A at 140 cd/m^2. This device contained a lithium-doped electron transport layer, two emissive layers, a spin-coated polyethylene dioxythiophene-polystyrene sulfonate (PEDOT:PSS) anode buffer layer, and a radio-frequency magnetron sputtered ITO anode.[12]

Here, we report on highly efficient green-emitting electrophosphorescent top-emitting OLEDs with Al/LiF bottom cathodes. Devices containing only two organic layers yield a current efficacy of 60.6 cd/A at a luminance of 1073 cd/m^2 when fabricated on a glass substrate. It has been previously shown that an organic capping layer on the semitransparent electrode of a top-emitting OLED can improve the outcoupling efficiency of the device by modifying the device's optical structure.[15] The current efficacy of our devices was increased to 92.5 cd/A at a luminance of 1300 cd/m^2 with the addition of an N,N′-Di-[(1-naphthyl)-N,N′-diphenyl]-(1,1′-biphenyl)-4,4′-diamine (α-NPD) optical outcoupling layer. Devices with such an outcoupling layer were also demonstrated on flexible polyethersulfone (PES) substrates and yielded a current efficacy of 96.3 cd/A at a luminance of 1387 cd/m^2.

Glass micro-slides (VWR international) and PES sheets were cut into 1 × 1 in. squares and used as substrates for the inverted top-emitting OLEDs. The glass substrates were sequentially cleaned by ultrasonication in baths of detergent water, distilled water, acetone, and isopropanol for 20 min each and then blown dry with nitrogen. PES substrates were cleaned and dried by the same process excluding cleaning

with acetone. The dry glass and PES substrates were treated by oxygen plasma for 2 min and 5 s, respectively. A layer of PEDOT:PSS Clevios P VP AI 4083 was dispensed through a 0.45 μm polyvinylidine fluoride filter and spin-coated at a speed of 5000 rpm for 1 min. The substrates were then annealed at 140 °C for 10 min. The thickness of the PEDOT:PSS was 40 nm and measured by spectroscopic ellipsometry. This layer planarizes the substrate and provides good wetting for the subsequent aluminum deposition. A previous report demonstrated that PEDOT:PSS on glass improves the reliability of electron-dominated organic diodes.[16] Including this layer also improves the yield and reliability of our inverted top-emitting OLEDs.

The samples were then transferred to a high-vacuum thermal evaporation system (EvoVac, Armstrong Engineering Inc.). The OLEDs on either glass or PES substrates were fabricated as separate batches. For all substrates, an aluminum layer of 50 nm was first deposited at a rate of 2 Å/s followed by a LiF electron-injection layer of 2.5 nm at a rate of 0.2 Å/s. All subsequent organic layers were deposited at a rate of 1 Å/s. A 40 nm-thick layer of 1,3,5-tri (p-pyrid-3-yl-phenyl)benzene (TpPyPB) was used as an electron transport material. The emissive layer was comprised of a 6 vol. % tris(2-phenylpyridine)iridium(III) $Ir(ppy)_3$ dopant coevaporated in a 20 nm layer of 4,4′-bis(N-carbazolyl)-1,1′-biphenyl (CBP). A 35 nm hole transport layer of CBP was then deposited. This was followed by a 15 nm-thick layer of molybdenum trioxide (MoO_3) deposited at a rate of 0.2 Å/s as a hole-injection layer. Finally, a 20 nm-thick top Au anode was deposited at a rate of 2 Å/s. The typical OLED area was 4×5 mm. To improve the optical outcoupling, an additional 120 nm-thick layer of α-NPD was deposited on top of the anodes of some devices for comparison. All depositions were performed at pressures below 3×10^{-7} Torr. All materials were purchased from Sigma-Aldrich except for TpPyPB and $Ir(ppy)_3$, which were purchased from Luminescence Technology Corporation. The organic materials were purified by gradient-zone sublimation.

After fabrication, the devices were transferred in a sealed nitrogen-containing vessel to another glove box where current-voltage and luminance-voltage characteristics were measured with a Keithley 2400 SourceMeter and a calibrated photodiode (FDS 100 from Thorlabs, Inc.). Electroluminescent spectra were measured with a radiometrically calibrated Ocean Optics USB4000 spectrometer.

Figure 1 shows a plot of the current density versus voltage of the OLEDs. Devices A and B are on glass substrates. Device A has no optical outcoupling layer and device B has an outcoupling layer of 120 nm of α-NPD. The current density versus voltage curves for both devices A and B are nearly identical, showing that the optical outcoupling layer had no effect on the electrical properties of the devices. In a separate batch, OLEDs were made on PES substrates also with an outcoupling layer of 120 nm of α-NPD (device C). As shown in Figure 1, these devices burned out at a lower driving voltage than devices A and B.

Figure 2 shows the luminance and current efficacy curves versus voltage. The turn-on voltages, maximum current efficacy, and maximum luminance of devices A, B, and C are summarized in Table I. The device performance of OLEDs on glass substrates has been verified in four separate batches with multiple OLEDs per batch. The average performance and standard deviation of OLEDs from these separate batches are shown in Table II.

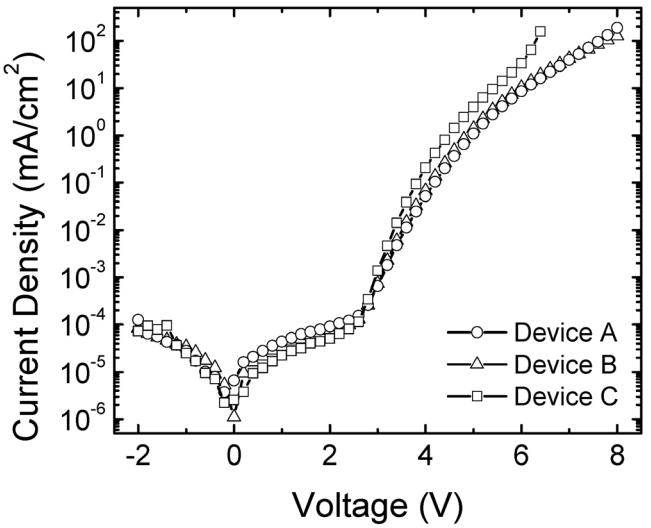

FIG. 1. Current density versus voltage curves for OLEDs with device structure: Substrate/PEDOT:PSS/Al/LiF/TpPyPB/CBP:Ir(ppy)$_3$/CBP/MoO_3/Au. Glass substrates were used for devices A (circles) and B (triangles), with device B having a 120 nm α-NPD optical outcoupling layer. Device C was fabricated on PES and also had an outcoupling layer.

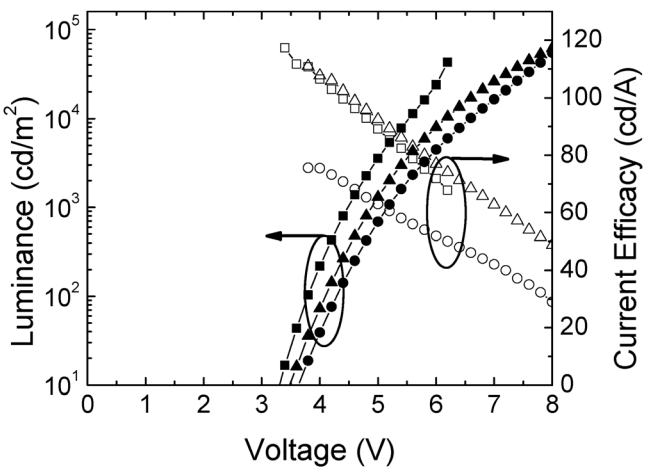

FIG. 2. Luminance and current efficacy versus voltage of device A (circles) and device B (triangles) on glass without and with an α-NPD optical outcoupling layer, respectively. Also shown is device C (squares) fabricated on a PES substrate and also having an outcoupling layer.

These results demonstrate that using a bottom Al/LiF cathode in conjunction with an electron transport layer of

TABLE I. Performance parameters of devices A (on glass with no optical outcoupling), B (on glass with outcoupling), and C (on PES with outcoupling). The turn-on voltage is defined as the voltage at a luminance of 10 cd/m^2.

	Turn-on voltage [V]	Max current efficacy [cd/A]	Max luminance [mA/cm^2]
Device A	3.6	75.6 (19.0 cd/m^2)	54,656 (29.0 cd/A)
Device B	3.5	111.0 (36.0 cd/m^2)	61,819 (48.8 cd/A)
Device C	3.3	117.0 (16.7 cd/m^2)	43,019 (67.9 cd/A)

TABLE II. Average performance with standard deviation for OLEDs on glass substrates. The data is taken from four separate batches.

	Luminance [cd/m^2]	Voltage [V]	Current density [mA/cm^2]	Current efficacy [cd/A]
Device A (6 devices)	100	4.3 (±0.1)	0.23 (±0.04)	58 (±7)
	1,000	5.2 (±0.1)	2.4 (±0.6)	53 (±5)
	10,000	6.7 (±0.2)	29 (±6)	42 (±8)
Device B (11 devices)	100	3.9 (±0.2)	0.11 (±0.02)	108 (±2)
	1,000	4.7 (±0.2)	1.5 (±0.1)	94 (±7)
	10,000	5.8 (±0.3)	15 (±2)	76 (±2)

TpPyPB and an anode of MoO_3/Au can lead to efficient inverted phosphorescent OLEDs, despite the cathode deposition order being the reverse of what is commonly used in conventional OLEDs. In addition, the MoO_3/Au semitransparent anode can inject holes directly into the highest occupied molecular orbital (HOMO) of the CBP host (6.3 eV)[17] without necessitating a different hole transport material with a lower HOMO level. Using CBP as a hole-transport layer has the additional benefits of reducing the number of different materials needed, as well as eliminating an organic-organic heterojunction of dissimilar materials. Furthermore, it is likely that the high efficiency of the OLED is promoted by a combination of desirable properties of the electron transport material, TpPyPB: its lowest unoccupied molecular orbital (LUMO) energy (3.04 eV) for enhancing electron injection, a HOMO energy (6.66 eV) for confining holes to the emissive layer, and a high electron mobility ($7.9 \times 10^{-3}\,cm^2\,V^{-1}\,s^{-1}$) as measured by time-of-flight experiments.[18]

To compare the effectiveness of injecting electrons from a bottom and top Al/LiF cathode, electron-dominated devices were fabricated. The device structure consisted of Glass/PEDOT:PSS (40 nm)/Al (50 nm)/LiF (2.5 nm)/TpPyPB (95 nm)/LiF (2.5 nm)/Al (50 nm). The HOMO level of TpPyPB ensures that hole injection from the Al/LiF electrodes is negligible. Current density versus voltage curves of these devices are shown in Figure 3, in which negative voltages and positive voltages correspond to electron injection from the bottom and top electrodes, respectively. The curve shows a slightly higher current (by less than one order of magnitude) when electrons are injected from the top electrode. This asymmetry could be the result of aluminum diffusion into the organic when the top electrode is deposited. Also shown is a comparison between identical electron-dominated devices where some have been subjected to a vacuum break and subsequently exposed to the glovebox N_2 atmosphere ($O_2 < 0.1$ ppm, $H_2O < 3.0$ ppm) after the bottom Al/LiF cathode deposition. The current density of the exposed devices decreases by nearly four orders of magnitude when electrons are injected from the bottom. It is possible that the Al/LiF cathode oxidizes when exposed to the trace amounts of O_2 and H_2O in the glovebox atmosphere. If an oxide forms, the insulating property of the oxide may reduce the ability of the cathode to inject electrons. Moreover, an oxide may prevent a chemical reaction from occurring between the ternary system of

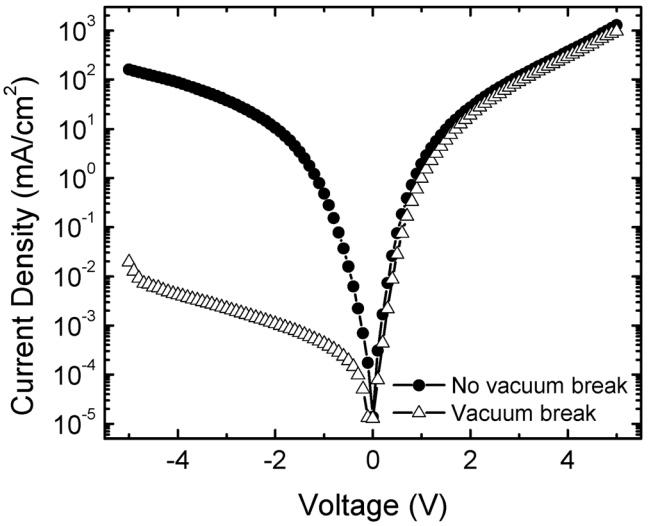

FIG. 3. Current density versus voltage characteristics of Al/LiF/TpPyPB/LiF/Al electron-dominated devices. Electrons are injected from the top electrode in forward bias and from the bottom in reverse bias. A vacuum break after deposition of the bottom Al/LiF results in a decrease of current density as high as four orders of magnitude when electrons are injected from the bottom electrode.

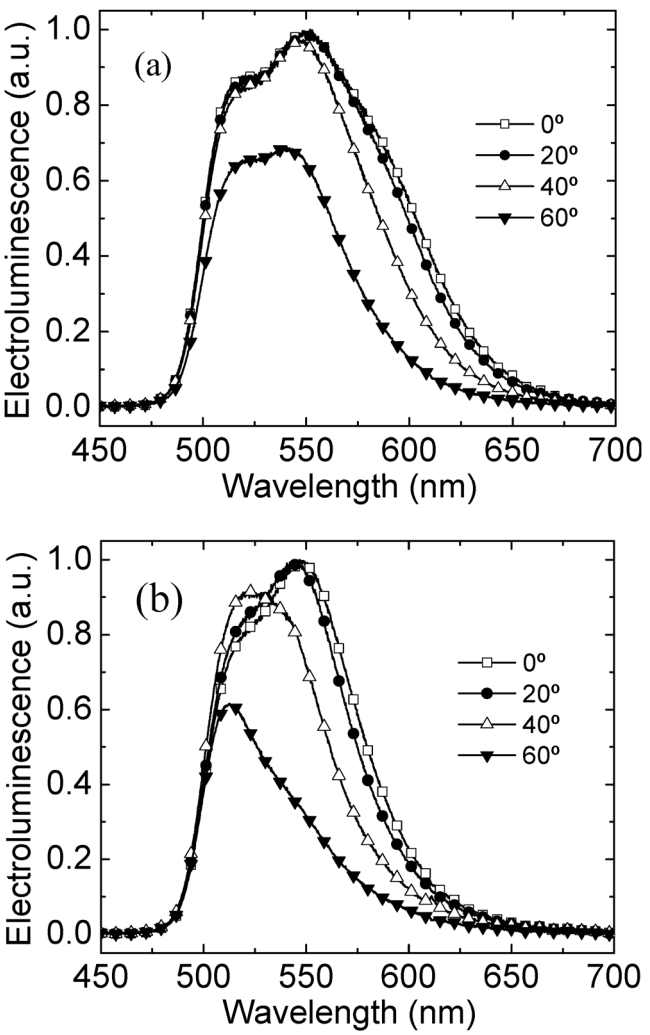

FIG. 4. (a) Electroluminescent intensity of device A and (b) device B measured at 20° increments from the surface normal. The measurements are normalized to the maximum intensity of the 0° spectrum.

Al/LiF/TpPyPB. Such a reaction has been shown to occur between Al/LiF/Alq_3 resulting in enhanced injection due to the presence of Alq_3^- radical anions.[19,20] The high sensitivity of the Al/LiF cathode to trace amounts of O_2 and H_2O may also explain why such cathodes have not been widely implemented in inverted OLED structures.

Figure 4 shows the angular electroluminescent spectra of both devices A and B taken at 20° increments from the surface normal. The spectra are normalized to the peak of the spectrum taken normal to the surface. The microcavity formed by the Al and Au layers[21] causes the spectra to narrow and shift with increasing angle causing the color of the OLED to change with the angle-of-view. The CIE coordinates (x, y) of device A are (0.38, 0.58) at 0° and shift to (0.31, 0.64) at 60°. The addition of the optical outcoupling layer leads to stronger shifting and narrowing of the spectrum. For device B, the CIE coordinates at 0° are (0.33,0.62) and shift to (0.26,0.65) at 60°.

OLEDs with microcavities cannot be assumed to be Lambertian emitters.[22,23] Therefore, the external quantum efficiency and power efficacy of the devices cannot be calculated from a single measurement of the luminance in the direction normal to the surface. One way to measure accurate values for these parameters is to capture all of the light emitted into the forward hemisphere using an integrating sphere. Accurately measuring these quantities will be the focus of future work.

In conclusion, highly efficient phosphorescent top-emitting inverted OLEDs have been demonstrated using a bottom Al/LiF cathode and an electron transport layer of TpPyPB. The OLEDs have a simplified structure containing only two organic layers. On glass, a current efficacy of 60.6 cd/A at a luminance of 1073 cd/m^2 was obtained. This current efficacy was shown to increase to 92.5 cd/A at a luminance of 1300 cd/m^2 with the addition of an α-NPD optical outcoupling layer. Devices on PES substrates and also having an outcoupling layer show a current efficacy of 96.3 cd/A at a luminance of 1387 cd/m^2. Future work will be focused on measuring the power efficacy of the devices using an integrating sphere.

This material is based upon work supported by the STC Program of the National Science Foundation under Agreement No. DMR-0120967.

[1]C. W. Tang and S. A. Vanslyke, Appl. Phys. Lett. **51**(12), 913 (1987).
[2]M. G. Helander, Z. B. Wang, J. Qiu, M. T. Greiner, D. P. Puzzo, Z. W. Liu, and Z. H. Lu, Science **332**(6032), 944 (2011).
[3]J. S. Kim, P. K. H. Ho, N. C. Greenham, and R. H. Friend, J. Appl. Phys. **88**(2), 1073 (2000).
[4]T. Dobbertin, M. Kroeger, D. Heithecker, D. Schneider, D. Metzdorf, H. Neuner, E. Becker, H. H. Johannes, and W. Kowalsky, Appl. Phys. Lett. **82**(2), 284 (2003).
[5]T. Dobbertin, O. Werner, J. Meyer, A. Kammoun, D. Schneider, T. Riedl, E. Becker, H. H. Johannes, and W. Kowalsky, Appl. Phys. Lett. **83**(24), 5071 (2003).
[6]C. W. Chen, C. L. Lin, and C. C. Wu, Appl. Phys. Lett. **85**(13), 2469 (2004).
[7]M. Thomschke, S. Hofmann, S. Olthof, M. Anderson, H. Kleemann, M. Schober, B. Lussem, and K. Leo, Appl. Phys. Lett. **98**(8), 083304 (2011).
[8]S. F. Chen, L. L. Deng, J. Xie, L. Peng, L. H. Xie, Q. L. Fan, and W. Huang, Adv. Mater. **22**(46), 5227 (2010).
[9]C. C. Wu, C. W. Chen, C. L. Lin, and C. J. Yang, J. Disp. Technol. **1**(2), 248 (2005).
[10]K. H. Kim, S. Y. Huh, S. M. Seo, and H. H. Lee, Org. Electron. **9**(6), 1118 (2008).
[11]Q. Wang, F. X. Wang, X. F. Qiao, and D. G. Ma, Semicond. Sci. Technol. **24**(10), 105027 (2009).
[12]M. Kroger, T. Dobbertin, D. Schneider, T. Rabe, E. Becker, H. H. Johannes, and W. Kowalsky, Proc. SPIE **5519**, 143 (2004).
[13]T. Matsushima, K. Goushi, and C. Adachi, Chem. Phys. Lett. **435**(4–6), 327 (2007).
[14]L. S. Hung, C. W. Tang, and M. G. Mason, Appl. Phys. Lett. **70**(2), 152 (1997).
[15]Q. Huang, K. Walzer, M. Pfeiffer, K. Leo, M. Hofmann, and T. Stubinger, J. Appl. Phys. **100**(6), 064507 (2006).
[16]R. Steyrleuthner, S. Bange, and D. Neher, J. Appl. Phys. **105**(6), 064509 (2009).
[17]A. Kahn, N. Koch, and W. Y. Gao, J. Polym. Sci. B-Polym. Phys. **41**(21), 2529 (2003).
[18]S. J. Su, T. Chiba, T. Takeda, and J. Kido, Adv. Mater. **20**(11), 2125 (2008).
[19]M. Mason, J. Appl. Phys. **89**(5), 2756 (2001).
[20]K. R. Choudhury, J. H. Yoon, and F. So, Adv. Mater. **20**(8), 1456 (2008).
[21]S. Hofmann, M. Thomschke, P. Freitag, M. Furno, B. Lussem, and K. Leo, Appl. Phys. Lett. **97**(25), 253308 (2010).
[22]J. Lee, S. Hofmann, M. Furno, M. Thomschke, Y. H. Kim, B. Lussem, and K. Leo, Org. Electron. **12**(8), 1383 (2011).
[23]S. Hofmann, M. Thomschke, B. Lussem, and K. Leo, Opt. Express **19**(23), A1250 (2011).